Research Square

Preprints are preliminary reports that have not undergone peer review.
They should not be considered conclusive, used to inform clinical practice,
or referenced by the media as validated information.

Overlying Soil Explosion on Reinforced Concrete Beams: Size Effect and Scaling Thresholds

Runze Cai

cairunze@cugb.edu.cn

China University of Geosciences (Beijing) https://orcid.org/0000-0003-2339-7971

Shaohua Cao

Chunxiao Zhang

Article

Keywords: Size effect, overlying soil explosion, reinforced concrete beam, stress-strain, damage pattern

Posted Date: May 20th, 2026

DOI: https://doi.org/10.21203/rs.3.rs-9495690/v1

License: This work is licensed under a Creative Commons Attribution 4.0 International License.
Read Full License

Additional Declarations: There is **NO** Competing Interest.

Overlying Soil Explosion on Reinforced Concrete Beams: Size Effect and Scaling Thresholds

Shaohua Cao[a,b,c], Chunxiao Zhang[abc], Runze Cai[*d]

[a]*State Key Laboratory of Target Vulnerability Assessment, Luoyang 471023, China*

[b]*Engineering Protection Research Department, DEI, AMS, Luoyang 471023, China*

[c]*Henan Key Laboratory of Special Protective Materials, Luoyang 471023, China*

[d]*School of Engineering and Technology, China University of Geosciences (Beijing), Beijing 100083, PR China*

Corresponding author: Cai Runze Email: cairunze@cugb.edu.cn

Abstract: The size effect of concrete, particularly in reinforced concrete (RC) beams subjected to overlying soil explosions, has yet to be fully clarified. A comprehensive understanding of this effect is crucial for extrapolating results from scale model tests to assess real-world damage in underground structures exposed to such explosions. This research aims to examine the size effect by conducting 17 overlying soil explosion tests on RC beams. The results indicate that the damage patterns, stress-strain behavior and mid-span displacement of RC beams exhibit a pronounced size effect, with smaller specimens exhibiting fewer cracks and reduced deformation. Furthermore, at a consistent scaled distance, the explosive pressure on RC beam surfaces differs due to the soil's energy absorption properties. In laboratory testing, the scale ratio of RC beams should exceed 1/4 of the actual structure to accurately simulate the effects of overlying soil explosions, and special consideration should be given to the errors in mid-span deflection. Finally, finite element analysis should recalibrate concrete parameters for different sizes to mitigate the size effect.

Key words: Size effect; overlying soil explosion; reinforced concrete beam; stress-strain; damage pattern.

1. Introduction

The size effect, also referred to as the size-dependent phenomenon, relates to the variation in nominal strength as the structural dimensions change [1]. Concrete, the most widely used material in engineering structures, has been extensively confirmed through experiments and theoretical studies to exhibit a significant size effect [2-4]. This effect primarily stems from the nonlinear modification of the fracture process zone (FPZ) as the structure scales up, largely due to the heterogeneous nature of concrete [5]. With the rapid advancement of society, the use of large-span beams in engineering structures has become increasingly common. However, financial constraints and limited laboratory space often necessitate testing scaled specimens, which presents challenges in accurately extrapolating the test results to reflect the mechanical response of full-scale structures.

Due to the limitations in test conditions and costs, current relevant research work is primarily focused on concrete material testing; for example, the aggregate size effect parameters of concrete materials have been the subject of extensive research under quasi-static loading conditions. As early as 1998, Zhou et al. [6] carried out experiments on concrete samples containing various types of aggregates to investigate the impact of size on nominal strengths. The results clearly revealed a size effect on nominal strengths in high-strength concrete with different aggregates. Similarly, Zheng et al. [7] developed five mesoscopic models to examine the impact of aggregate gradation and specimen side length on concrete compressive strength. Their findings demonstrated a noticeable decline in compressive strength as the maximum aggregate size increased. In contrast, Liu et al. [8] explored the size effect on tensile strength in lightweight aggregate concrete, concluding that the gradation of concrete had a relatively negligible impact on the size effect. The result contradicts the implicit correlation between aggregate characteristics and size effect observed in Zheng et al. [7]. Jin et al. [9] further extended this line of research to reinforced concrete (RC) beams, analyzing the impact of concrete strength and aggregate size on the size effect of shear capacity. Their findings revealed that larger aggregate sizes enhanced the shear strength of joints, while smaller aggregates led to reduced ductility; notably, the size effect became more pronounced as aggregate size decreased, which aligns

with Zhou et al. [6] observation of size effect sensitivity to aggregate properties but also underscores the need to contextualize size effect mechanisms within structural components (e.g., beams) rather than just bulk concrete.

1.1. Size effect of RC beams under static loading

Previous research has primarily focused on the size effect of RC beams under static loading, with consistent findings that RC beams exhibit a distinct size effect-though critical differences exist in the mitigating factors identified across studies. For instance, Yang et al. [10] conducted shear experiments on RC beams to investigate the influence of web steel and beam depth on the size effect. They found that the presence of web steel in deep beams helped reduce the size effect by strengthening concrete struts and enhancing boundary confinement, but it could not completely eliminate the effect. In contrast, Cucuzza [11] focused on the sensitivity of beam response to fracture energy and found that estimated fracture energy varied with beam size, this suggests that the size effect in static loading is not only governed by structural reinforcement (as highlighted by Yang et al. [10]) but also by material fracture properties, creating a limitation in understanding how these two factors interact to regulate size-dependent behavior. Lei et al. [12] explored the size effect of torsional resistance in RC beams, showing that torsional resistance and ductility decrease with increasing beam size, and stirrups can improve torsional strength and reduce torsional size effect. This finding parallels Yang et al. (2025) observation that reinforcement mitigates size effects but also reveals that the effectiveness of reinforcement depends on the loading type. Fan et al. [13] further validated the static size effect by conducting shear experiments on high-strength concrete beams with depths ranging from 450 mm to 1800 mm and spans from 4000 mm to 13400 mm. Their results indicated that ultimate shear strength decreased with increasing beam depth, attributed to more extensive flexural and shear cracking in larger beams, consistent with the FPZ modification mechanism proposed earlier but also emphasizing that static size effect magnitude is strongly dependent on beam geometry.

1.2. Size effect of RC beams under dynamic loading

In addition to being exposed to static loads throughout their operational life, concrete structures are

occasionly subjected to dynamic loads such as seismic activity, wind, impact, and explosions [14-16]. These dynamic loads are typically the most critical considerations in the design of concrete structures due to their unpredictability and potential for significant damage. Concrete, as a rate-dependent brittle material, displays much higher dynamic strength compared to its quasi-static strength [17]. Existing research on the size effect of RC beams under dynamic loads remains fragmented and incomplete, with conflicting findings and limited coverage of extreme dynamic scenarios. Therefore, it is essential to explore the size effect on the dynamic mechanical behaviour of RC beams to ensure the validity of laboratory scaling test results. Cheng et al. [18] conducted fast loading tests on RC beams with the maximum loading velocity of 2.0 m/s, revealing the failure mode of RC beams changed from bending failure to shear failure as the predominant mode. Jin et al. [19] also found that the shear capacity of RC beams increased with the increase of strain rate, resulting in a weakening of the size effect in shear failure. Park et al. [20] discovered that the bending capacity of RC beams was mainly affected by kinetic energy rate and beam size. Nearly all dynamic size effect studies on RC beams have focused on impact or seismic loading, with minimal attention to blast loading-especially overlying soil explosions, which are common in underground civil defense and military structures but have been largely overlooked.

1.3. Scope of the present study

As mentioned above, current research on the size effect of reinforced concrete under dynamic loads, particularly under blast impact loading, remains insufficient. Although our previous paper [21] and Cheng et al. [18] investigated the size effect of reinforced concrete slabs under contact explosion, a notable gap persists in understanding the size effect of RC beams under overlying soil explosions. This research gap is particularly problematic for underground civil defense engineering and military installations (e.g., underground command centers, bunkers), where RC beams are critical structural components subjected to overlying soil explosions, and laboratory-scaled tests are the primary means of evaluating explosion resistance. Without understanding the size effect under this specific loading condition, scaled test results cannot be reliably extrapolated to full-scale structures, posing significant risks to structural safety and design validity.

To address this critical research gap and justify the specific focus on overlying soil explosions, this study aims to explore the size effect of RC beams under overlying soil explosions, examining variations in steel compressive/tensile strain, concrete compressive strain, and mid-span displacement. Scaled specimens adhere to full-size geometric scaling principles, incorporating parameters such as maximum aggregate diameter, beam span, rebar diameter and spacing, support width, and explosive charge. Furthermore, a finite element (FE) comparative analysis is conducted to evaluate compressive strain and damage patterns between scaled and full-size specimens. The Jones-Wilkins-Lee (JWL) is applied to simulate the effects of overlying soil explosion on the finite element modeled RC beams at a consistent scaled distance. By combining experimental results with FE analysis, this study addresses the existing knowledge gap concerning size effects under explosions involving overlying soil. It establishes a foundation for selecting appropriate scale ratios for reinforced concrete beams under such critical loading conditions, thereby directly supporting the design of underground structures and the evaluation of their blast-resistant performance.

2. Experiment design

2.1. Test specimens

Three types of RC beams, each with different spans, were prepared and subjected to overlying soil explosion tests, with the cross-sectional dimensions shown in Fig. 1. The spacing between the 11 stirrups in the 3 m beam was 288 mm, with proportional scaling applied to the smaller beams. Due to the reduced spacing between rebars in the scaled beams, the maximum coarse aggregate size of 40 mm, commonly used in civil and military concrete mix designs, was unsuitable. Consequently, three custom-designed concrete mixes with smaller maximum aggregate diameters were developed, each with a cuboid compressive strength of 38 N/mm^2, as detailed in Table 1. The stress-strain curves for all three mixes were nearly identical. Further details on the concrete mix proportions can be found in this paper [21]. During specimen production, strict control was maintained over the placement of the reinforcement to ensure the geometric dimensions of the RC beams were accurate. The rebars were manually tied and secured, and a hand vibrator was employed to minize internal voids within the concrete. The specimens

were made with PO 42.5 cement, river sand, tap water and coarse granite aggregate with a size range of 5-20 mm. After demolding, the specimens were cured with 28 days preparation for the explosion tests.

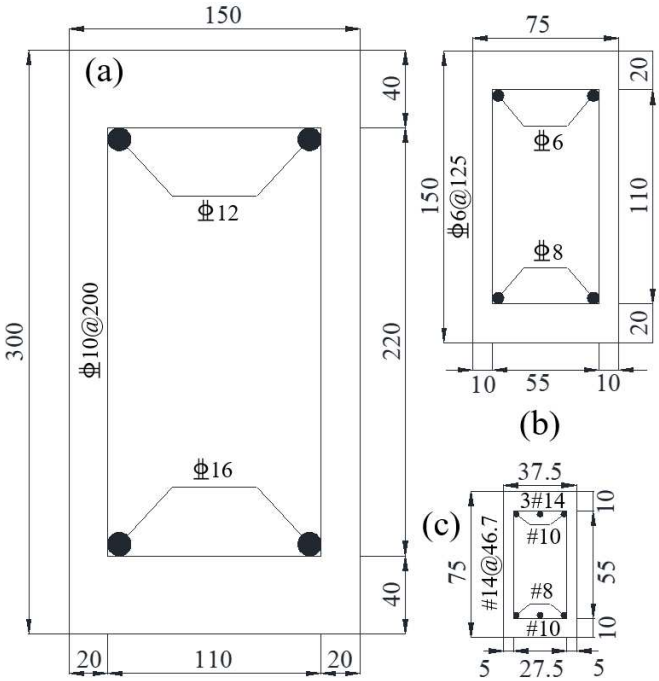


Fig. 1. Detailing of rebars in reinforced concrete beam (unit: mm).
(a) 3 m (b) 1.5 mm (c) 0.75 mm

Table 1
Concrete mix proportion.

No.	Configuration strength (N/mm^2)	Average value (N/mm^2)	Maximum aggregate diameter (mm)	Water-cement ratio	Amount of material (kg/m^3)			
					Water	Cement	Sand	Gravel
1#	38	38.3	5	0.48	222	462	601	1114
2#	38	38.2	10	0.49	215	439	584	1086
3#	38	38.0	20	0.44	195	443	599	1163

2.2. Test setup

As illustrated in Fig. 2, a standard TNT block measuring 100 mm × 50 mm × 25 mm and weighing 200 g was used for this experiment. The group charging method was adopted, positioning the TNT block at the center of the RC beam on the overlying soil. The block was detonated with a No. 8 electronic detonator, containing 1.07 g of TNT. The RC beams were simply supported by walls on a foundation, as depicted in Fig 3. Three different sizes of RC beams were considered: a full-size model (3.0 m span), a 1/2 scaled model (1.50 m span), and a 1/4 scaled model (0.75 m span), with corresponding support widths of 200 mm, 100 mm, and 50 mm, respectively.

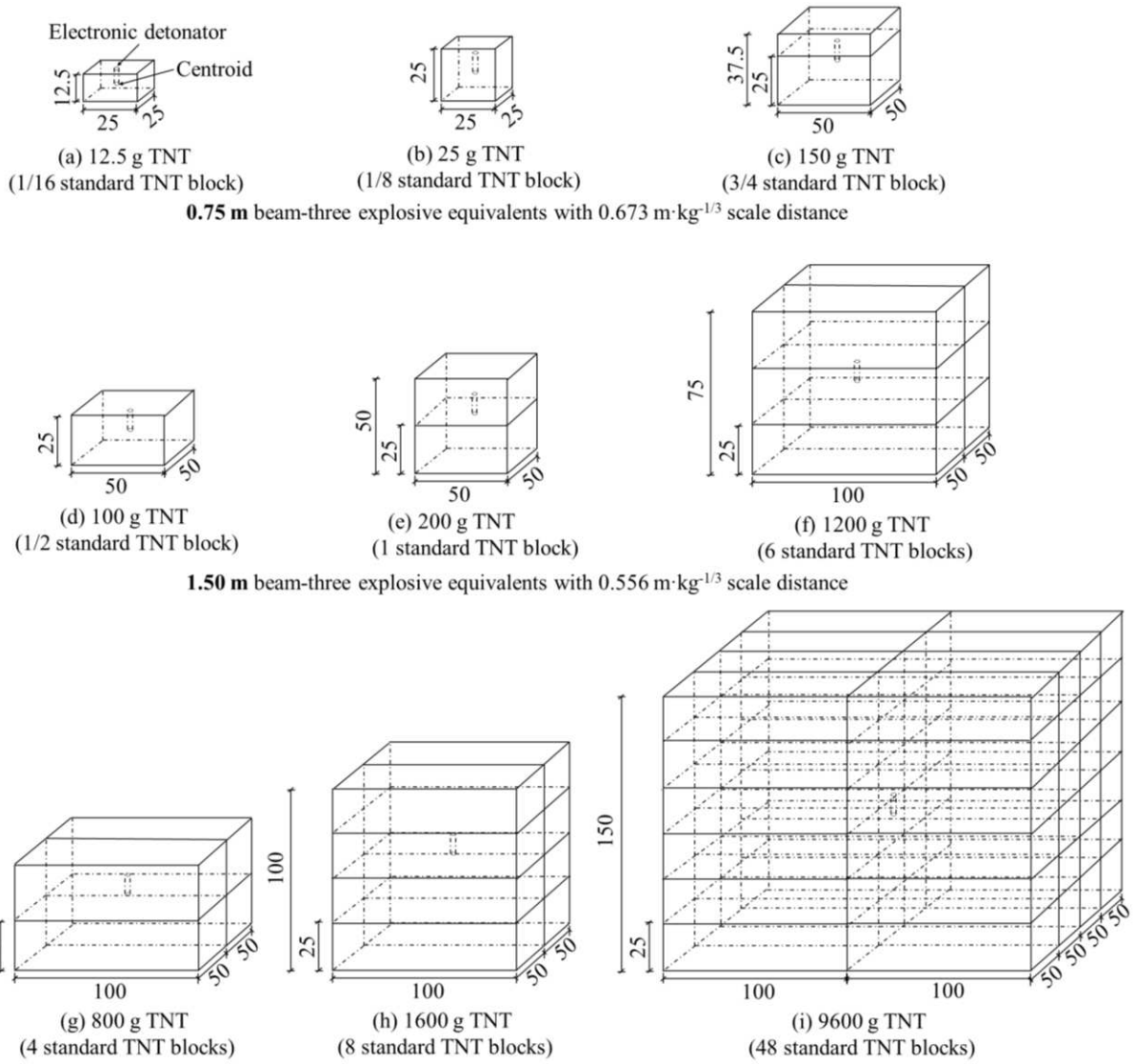


Fig. 2. The group charging method of TNT block (unit: mm).

To investigate the size effect of RC beams under various TNT equivalent explosions with overlying soil, tests were conducted using small, medium, and large charge weights. These charges were designed to simulate elastic, elastoplastic and plastic failure modes, respectively. Blast pressure time histories were recorded during the tests using pressure sensors. Ensuring the scaled explosives produced comparable impulse forces on the upper surface of the RC beam was critical, and the DH5922N dynamic signal test acquisition and analysis system was used to capture the explosion pressure data.



Fig. 3 Test arrangement. (a) before the blasting test. (b) after blasting test
(c) displacement meter (d) pressure sensor and strain gauge

Table 2
Geometric parameters of components.

No.	Span (m)	Width (m)	Thickness (m)	No.1 blast explosive charge (g)	No.2 blast explosive charge (g)	No.3 blast explosive charge (g)	Overlying soil thickness (mm)	Mix proportion
1-4	0.75	0.0375	0.075	12.5	25	150	150	1#
5-9	1.5	0.075	0.15	100	200	1200	300	2#
10-11	1.5	0.075	0.15	100	200	1200	300	3#
12-17	3	0.15	0.3	800	1600	9600	600	3#

Material	Yield strength (MPa)	Ultimate strength (MPa)	Elasticity modulus (GPa)	Density (kg/m^3)	Elongation (%)	Poisson ratio
HPB235	305	465	210	7800	30.5	0.3
HRB400	448	622	210	7800	26.5	0.3

Details of each specimen are listed in Table 2. By comparing No. 5-9 with No. 10-11, we sought to determine whether the aggregate size affected the damage level of RC beams during blasting, considering that the stress-strain curves displayed similar behaviors for different concrete mixtures of 1.5 m beam. Prior to the tests, a blast pit was constructed, with an observation room positioned at the base. For instance, the observation room for the 3 m beams was 3 m × 3 m × 2 m. The bottom plate was 0.05 m thick, and the side walls were 0.5 m thick, with all others dimensions proportionally scaled down

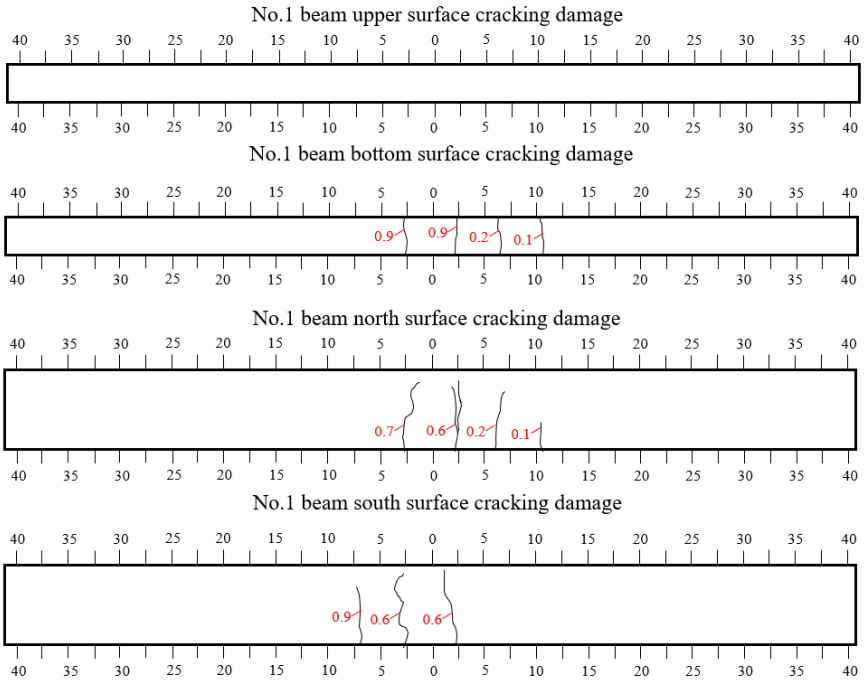
for smaller beams.

3. Experimental results

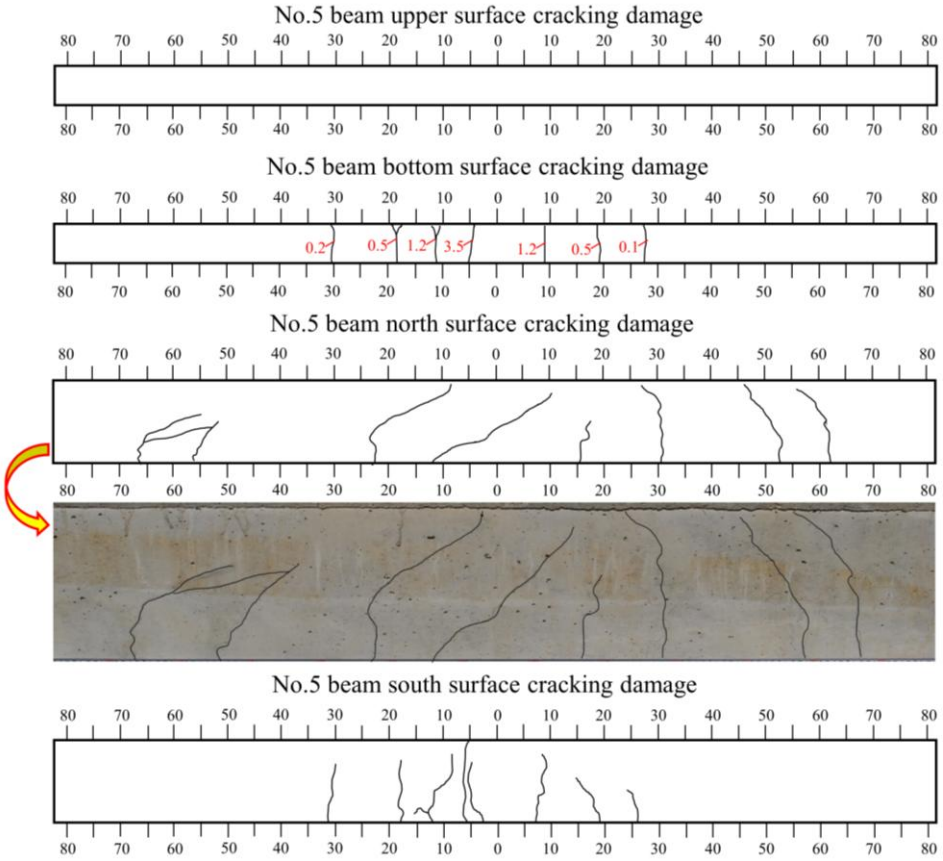
3.1. Cracking damage

Cracking damage patterns under various blast loads for each RC beam are depicted in Fig. 4, with additional details provided in the supplementary material. Analysis reveals that the extent of damage increases proportionally with the span of the beams. Full-sized specimens exhibit longer and wider cracks compared to scaled-down specimens. Additionally, spalling, defined as the detachment of concrete fragments from the surface, is observed in the full-sized specimens but absent in the scaled ones. This underscores the evident size effect exhibited by RC beams under overlying soil explosions. Cracks typically initiate at the bottom of the RC beams and propagate towards the upper surface, a phenomenon observable from both the southern and northern sides of the RC beams. The damage distribution in the RC beams aligns with the well-established principle that concrete structures possess greater resistance to compressive loads than tensile loads. thus the upper surfaces of the RC beams experience less damage, while the lower surfaces exhibit more severe damage. Bending damage is most pronounced at the mid-span, consistent with the descriptions in references [22, 23].

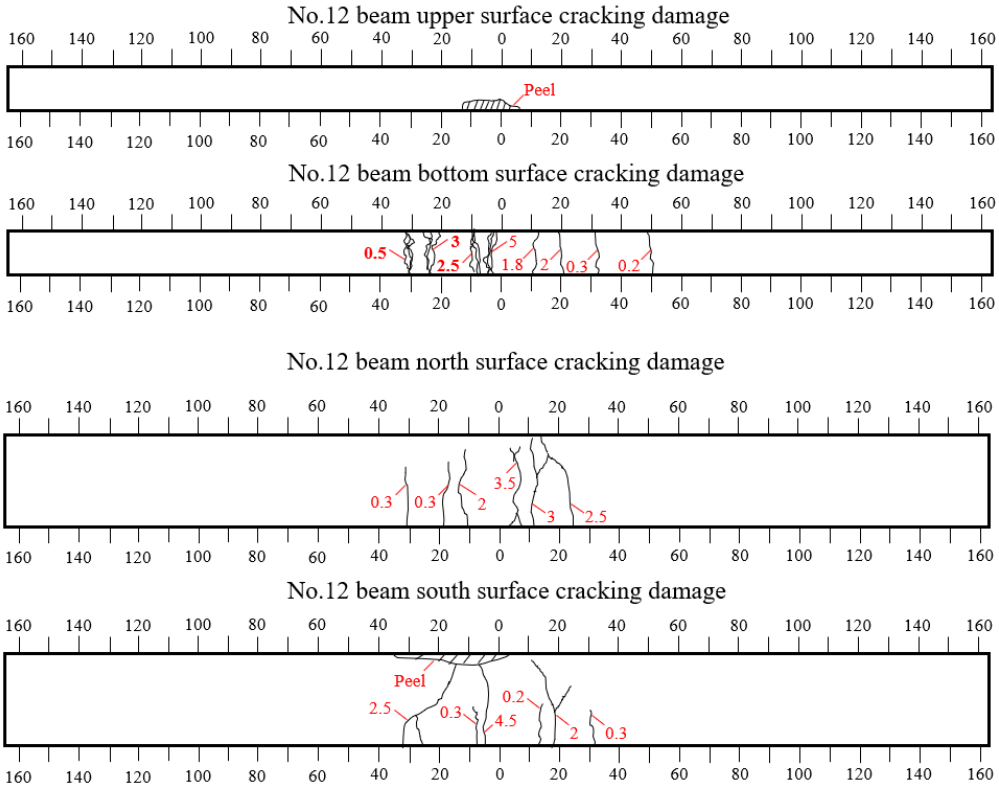
Despite the use of group charge arrangement, the overlying soil layer prevents the formation of an explosion crater on the upper surface of the RC beams. Additionally, the energy absorption by the soil layer mitigates the formation of a collapse crater at the bottom of the beam, resulting in only minor spalling damages. The blast shock wave acting on the upper surface of the RC beams is relatively uniform, which minimizes stress concentration. As a result, the damage observed in the RC beams is primarily bending-related, with a slight degree of shear damage. To mitigate tensile damage under blast loading, installing prestressed reinforcement at the bottom of the beam represents an effective solution [24].



(a) 0.75 m beam



(b) 1.5 m beam



(c) 3 m beam

Fig. 4 Cracking damage of each span under overlying soil explosive loads.

3.2. Compressive strain of rebar

Fig. 5 illustrates the compressive strain of rebar of the three RC beams with varying spans under small, medium and large equivalent blast impacts. The typical blast waveform for No. 2 blast is depicted in Fig. 5(a), and Fig. 5(b) summarizes the mean compressive strain values. As shown in Fig. 5(a), the duration of positive pressure increases with increasing beam span. Specifically, the positive pressure duration for the 0.75 m, 1.5 m and 3 m spans are 10.42 ms, 20.72 ms and 37.84 ms, respectively, showing close proportionality to span length. At proportional scaled distance, the compressive strain peak values of scaled models are supposed to be nearly identical to the full-sized ones. As shown in the tests, the compressive strain peak values for the 1.5 m and 3 m beams are approximately 253 με and 247 με, respectively. However, the compressive strain peak value for the 0.75 m beam is 1.2 times higher than that for the 1.5m and 3 m span beams, reaching 300 με.

Fig. 5(b) highlights the elastic deformation of RC beams in the No. 1 and No. 2 blast tests. Among the three tested beams, the 3 m beam exhibits the lowest compressive strain mean peak value, followed

by the 1.5 m and 0.75 m beams. This behavior can be attributed to the thinner overlying soil, which absorbs less energy from the blast impact and consequently exerts higher pressure on the 0.75 m beam. This trend is reflected in subsequent compressive strains of concrete. However, No. 3 blast pushes the beams beyond their elastic limit, resulting in substantial damage to the measurement points, and the compressive strain mean peak value in the 0.75 m beam becomes lower compared to the others. Despite modifications in the mix proportions of the 1.5 m beams, the measured compressive strain means peak values of the rebars remain relatively consistent.

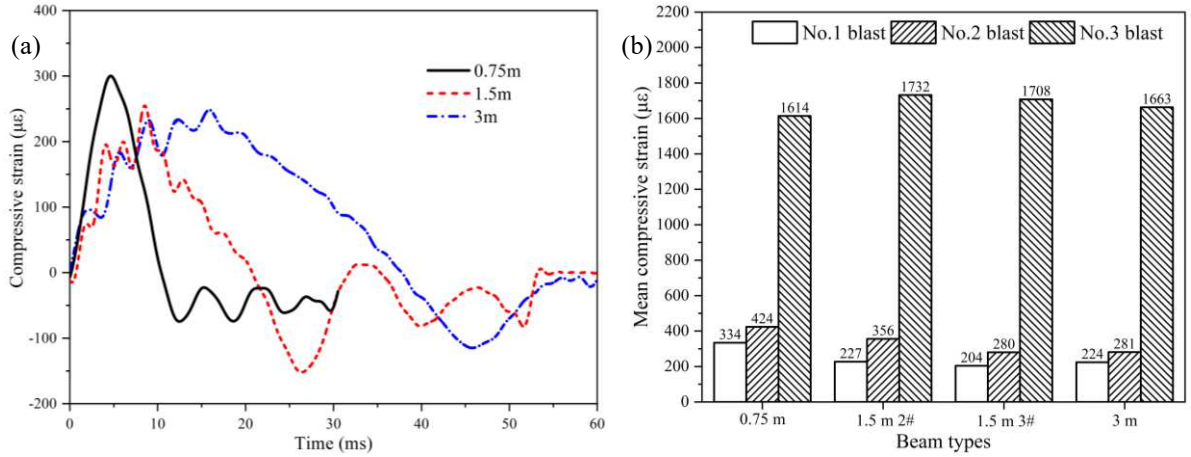


Fig. 5 Comparison of rebar compressive strain with different spans under blast impact. (a) No.2 blast typical waveform (b) mean peak value

3.3. Tensile strain of rebar

Fig. 6 shows the tensile strain response of rebar in each beam subjected to blast impact. Fig .6(a) and Fig. 6(b) represent the No. 2 typical blast waveform and tensile strain mean peak value respectively. As the beam span increases, the strain of the rebar in the tension zone of RC beams and the positive pressure duration increases, respectively. For example, the positive pressure duration for 0.75 m, 1.5 m and 3 m beams is shown in Figure 6(a) as 13.23 ms, 25.37 ms, and 39.09 ms, respectively. The positive pressure effect on the test specimen of the 0.75 m beam is significantly reduced, reaching only 33.8 % of that on the 3 m beam. From Fig. 6(b), it is evident that although the compressive strain in RC beams decreases with an increasing span, the tensile strain of the rebar increases. This phenomenon is due to the reduced explosive charge, which scales down with the beam span, resulting in a weaker blast that transmits less energy or impulse from the upper surface to the bottom surface. This observation is

supported by Patel and Patel [25]. It is worth noting that the tensile strains of the two mix proportions for the 1.5 m span RC beams are nearly identical. However, the tensile strain for the 3 m beam was significantly reduced in the No.3 blast. This can be attributed to the fact that the beam had entered the plastic failure stage, exhibiting visible spalling and numerous cracks on the bottom surface. These damages absorbed substantial shock wave energy, weakening the tensile strain in the rebar [26, 27].

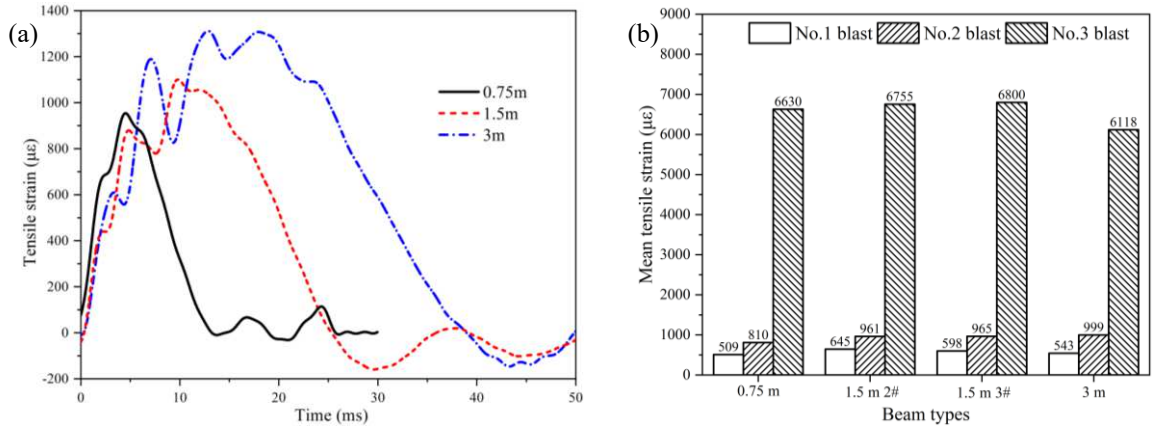


Fig. 6 Tensile strain of rebar under different equivalent blast.
(a) No.2 blast typical waveform (b) mean peak value

3.4. Compressive strain of concrete

The history curves of compressive strain of concrete under blast impact are illustrated in Fig. 7, with Fig.7 (a) showing the No. 2 typical blast waveform and Fig.7 (b) showing mean peak value of concrete tensile strain, respectively. As the beam span increases, the compressive strain peak value of concrete on the upper surface decreases and the positive pressure duration increases, as shown in Fig.7 (a). The positive pressure duration for 0.75 m 1.5 m and 3 m beams is 9.4 ms, 19.6 ms and 33.3 ms, respectively. These durations are approximately consistent with the trend of compressive strain of rebar, thus validating the accuracy of the obtained data. In the case of the 1.5 m span RC beams with two different concrete mix proportions, the compressive strains on their upper surface yield similar results. In Fig.7 (b), it is evident that the compressive strain of the concrete on the upper surface of the 3m span beam experiences a significant decrease, surpassing the compressive strain of the steel bar discussed earlier. This phenomenon can be attributed to the shorter duration of the explosion, which imposes a more intense impact force on the structure. As a result, the concrete becomes more brittle, leading to a

noticeable drop in compressive strain on the upper surface [28]. Cracks and fractures also occur before the concrete is completely deformed. such phenomena absorb substantial shock wave energy, thus weakening damage to the upper surface.

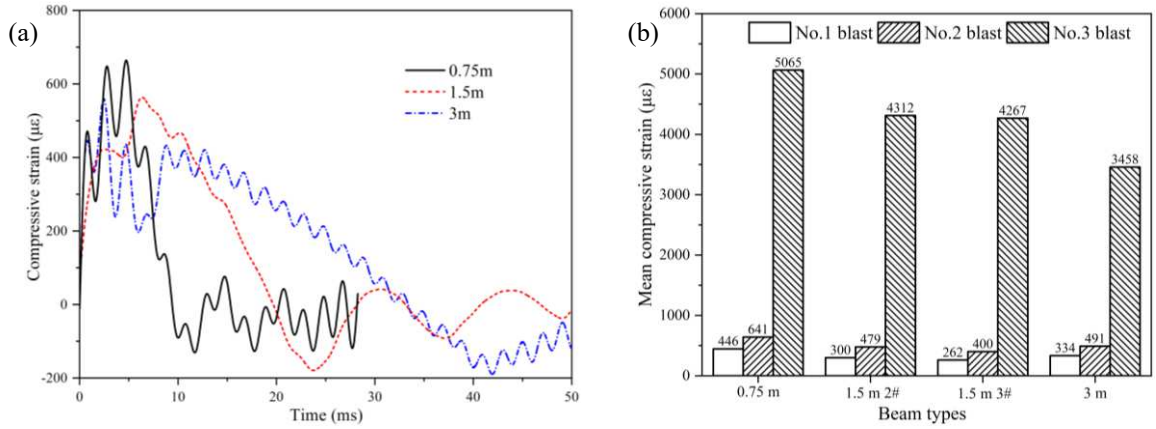


Fig. 7 Compressive strain of concrete under different equivalent blast.
(a) No.2 blast typical waveform (b) mean peak value

3.5. Mid-span displacement

Fig. 8 illustrates the comparison of mid-span displacement among three types of RC beams subjected to three different blast loads at a consistent scaled distance. The residual displacement is employed as a metric to assess the size effect of RC beams under overlying soil explosion. As shown in Fig. 7(a), the mid-span displacement and residual displacement of RC beams increase with larger spans in the No.3 blast, consistent with the trend observed in the tensile strain of the rebar. The 3 m beam exhibits the largest residual displacement at 32.5 mm, followed by the 1.5 m beam at 5.3 mm, and the 0.75 m beam at 2.8 mm. The mid-span displacement of the 3 m beam is approximately 11.6 times greater than that of the 0.75 m beam, demonstrating a pronounced size effect. Fig.7 (b) further illustrates that mid-span displacement mean peak value of RC beams grows as the span increases at a consistent scaled distance. Such size effect becomes more obvious as the blast load intensity increases. Notably, the mid-span displacement of the 1.5 m span RC beams with two different concrete mix proportions shows minimal difference. It is widely recognized that explosives of varying weights generate the same positive pressure at a consistent scaled distance based on the Scaling Laws [29]. However, the above test results show that impact forces and the positive pressure duration differ in RC beams subjected to different

explosives weights at a consistent scaled distance under overlying soil explosion.

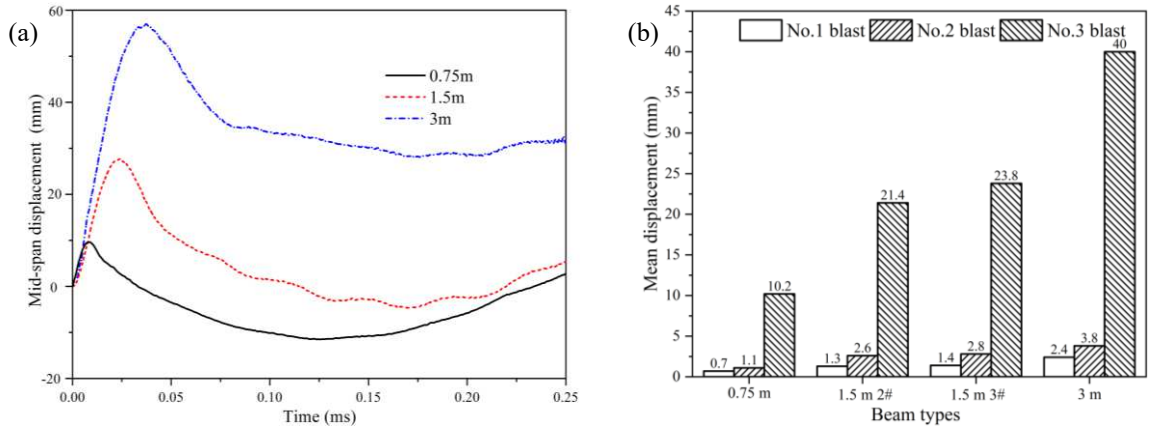


Fig. 8 Mid-span displacement of RC beam under different equivalent blast.
(a) No.3 blast typical waveform (b) mean value

3.6. Error analysis

Table 3 presents the percentage error used to compare the size effect on various factors such as rebar compressive strain, rebar tensile strain, concrete compressive strain, and mid-span displacement between scaled and full-size specimens. The errors attributed to the size effect are comprehensively summarized. While the force distribution in the scaled specimens may resemble that of their full-size counterparts, smaller structures are likely to exhibit fewer local damages and cracks in the blast tensile area. This is due to the reduced number of internal defects, such as microcracks and pores, in small structures, which may delay cracking and minimize subsequent damage when exposed to explosive forces [30]. Therefore, further research is crucial to fully comprehend the impact of size on the behavior of RC beams under overlying soil blast loads. These investigations are critical to achieve a more precise and comprehensive understanding of the size effect.

For all applied overlying soil blast loads, the mid-span displacement exhibits the highest error, followed by the compressive strain in both the concrete and rebar, with the least error observed in the rebar tensile strain. It is noteworthy that while a significant discrepancy exists in the compressive strain errors between the 0.75 m beam (1/4 scaled model) and the 3 m beam (full-size model), the error in data obtained from the 1.5 m beam (1/2 scaled model) remains minimal. For example, the compressive strain error of the 0.75 m beam is 49.1 %, compared to just 1.3 % for the 1.5 m beam. In the laboratory-scaled

tests of reinforced concrete beams (RC beams) subjected to overlying soil explosions, the 1/4 scaled model introduces a comprehensive error of nearly 40 %. However, to minimize these errors, particularly given the mid-span displacement error, which can reach nearly 70 %, it is critical to consider an error coefficient. The 1/2 scaled model, in contrast, presents a more manageable total error of approximately 20 %. Ultimately, the model selection should be guided by the acceptable error threshold in engineering analysis. The authors recommend that the scale ratio for overlying soil explosion tests should exceed 1/4 of the actual structure. Otherwise, the obtained data may lack significance beyond merely understanding stress distribution patterns.

Table 3
Scaled RC beams error analysis under overlying soil explosion.

Error (%)	No.1 blast			No.2 blast			No.3 blast		
	0.75 m	1.5 m 2#	1.5m 3#	0.75 m	1.5 m 2#	1.5m 3#	0.75 m	1.5 m 2#	1.5m 3#
Rebar compressive strain	49.1	1.3	-8.9	50.9	26.7	-0.4	-2.9	4.1	2.7
Rebar tensile strain	-6.3	18.7	10.1	-18.9	-3.8	-3.4	26.9	10.4	11.1
Concrete compressive strain	33.5	-10.2	-21.6	30.5	-2.4	-18.5	46.5	24.7	23.4
Mid-span displacement	-70.8	-45.8	-41.7	-71.1	-31.6	-26.3	-74.5	-46.5	-40.5
Mean	39.9	19.0	20.6	42.9	16.1	12.2	37.7	21.4	19.4

4. Numerical modelling

4.1. Geometry modelling

A high-fidelity physics-based 3D finite element (FE) model was developed using ABAQUS to analyze the mechanical behavior of RC beams subjected to overlying soil explosions. Eight-node brick solid elements (C3D8R) [31-33] were employed to model the concrete and soil, while was modelled using two-node truss elements (T3D2) [34-36] represented the internal reinforcement rebars. A consistent mesh size of 15 mm was applied across all elements to guarantee precision and accuracy in the structural modeling. To prevent unnecessary repetition not presented in this paper, mesh sensitivity analyses were conducted to determine the optimal mesh size. Observations reveal that further mesh refinement yielded similar simulations results but at the cost of increased computational time. The model assumed a perfect bond between the concrete and reinforcement bars, with zero stress applied at the free

ends of the beams to ensure full effective stress at the end of the transmission length [37]. The rebars were coupled with the concrete using the EMBEDDED_REGION constraint command [38]. Surface-to-surface kinematic contact was used to model the supports and RC beam, ensuring simple support for the RC beam. A fixed boundary condition was applied at the bottom surface of the supports, restricting all six degrees of freedom: three translational and three rotational.

4.2 Parameters selection

4.2.1. Concrete

The Concrete Damaged Plasticity (CDP) model is utilized to analyze the non-linear response of the concrete under explosive loading [39]. This model incorporates a plastic damage variable, which characterizes the development of failure surfaces caused by compression damage (d_c) and tension damage (d_t). These failure surfaces provide insight into how concrete deteriorates under compressive and tensile stresses [40]. The uniaxial stress-strain curve was calculated following the procedures outlined in the ABAQUS/CAE user manual [41], and the parameters of concrete CDP model are listed in Table 4. The stress-strain relationships for both compressive and tensile loading are as follows:

$$\sigma_c = (1-d_c)E_0\left(\varepsilon_c - \varepsilon_c^{pl}\right) \tag{1}$$

$$\sigma_t = (1-d_t)E_0\left(\varepsilon_t - \varepsilon_t^{pl}\right) \tag{2}$$

where E_0 is the initial (undamaged) elastic modulus of the concrete.

Table 4
Concrete CDP sensitive parameters [42].

Poisson's ratio	Dilatation angle	Flow potential eccentricity	f_{b0}/f_{c0}	K	Viscosity parameter
0.2	38°	0.1	1.16	0.6667	0

4.2.2. Rebar

The reinforcement bars, including the longitudinal bars and stirrups, are represented as elastic-plastic materials using the classical metal plasticity model [34]. In this model, the rebars within RC beam are considered isotropic, with plasticity governed by kinematic hardening. To address strain rate effects, the model proposed by Symonds [43] is utilized:

$$\frac{\sigma_d^{'}}{\sigma_s}=1+\left(\frac{\dot{\varepsilon}}{C}\right)^{1/P} \tag{3}$$

Where σ_d' is the dynamic flow stress, σ_s is the static flow stress, $\dot{\varepsilon}$ is the plastic strain rate, C and P are material constants. C=40, and P=5 [44]. The rebar parameters are detailed in Table 2.

4.2.3. Soil layer

The Drucker-Prager (DP) plasticity model is employed to represent the soil layer, as it is suitable for simulating soil materials under blast conditions [45]. The parameters of the DP model and other relevant mechanical properties are specified in Table 5. More details about DP plasticity model can be found in reference [46].

Table 5
DP and mechanical parameters [46].

Soil	Parameters	Symbol	Values
DP plasticity model	Friction angle	ϕ	30°
	Dilatancy angle	ψ	10°
	Yield surface shape parameter	K	0.8
	Initial yield strength	σ_y	100 kPa
Mechanics	Density	ρ	1,800 kg/m^3
	Modulus of elasticity	E	50 MPa
	Poisson's ratio	ν	0.3

4.2.4. TNT

The Jones-Wilkins-Lee (JWL) equation of state is employed to characterize the detonation behavior of TNT explosive:

$$P=A\left(1-\frac{\omega}{R_1V}\right)e^{-R_1V}+B\left(1-\frac{\omega}{R_2V}\right)e^{-R_2V}+\frac{\omega}{V}E \tag{4}$$

Where the equation defines the pressure P of detonation products as a function of the relative volume V *and initial internal energy* E=3680 kJ/kg. A=373.77 GPa, B=3.7471 GPa, R_1=4.15, R_2=0.9, ω=0.35 are constants pertaining to the explosive. Moreover, the density of the TNT explosive is 1.63×10^3 kg/m^3 [47].

4.3 Numerical models verification

Taking a RC beam as an example, Fig. 9 illustrates the concrete compressive strain in RC beams

with a 3 m span subjected to overlying soil explosions. The finite element (FE) analysis results demonstrate significantly higher values for the smaller equivalent explosion and slightly lower values for the larger equivalent explosion compared to experimental data. Table 6 presents a comparative evaluation of the peak values for RC beams with spans of 0.75 m and 3 m under the No.3 explosion test. The mean error for the 0.75 m RC beam is 12.1 %, while the mean error for the 3 m RC beam is 10.7 %. This discrepancy can be attributed to the presence of more internal defects and pores in the larger specimens [48]. However, as the FE analysis employs the same parameters for both cases, the influence of the size effect cannot be adequately considered.

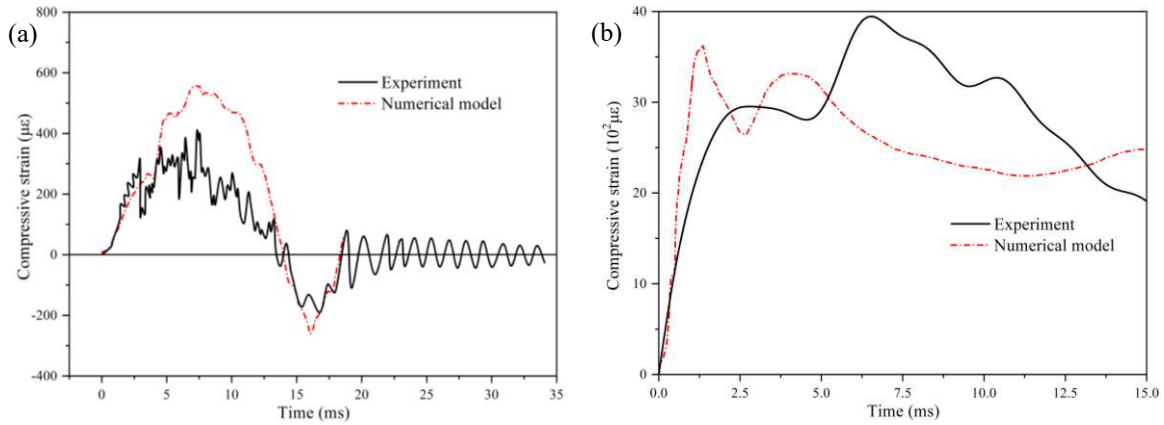


Fig. 9 Comparison of concrete compressive strain between test and FE simulation. (a) No.1 blast (b) No.3 blast

Table 6
Comparation of peak values between FE and experiment.

Parameters	Symbol	0.75 m			3 m		
		FE	Experiment	Error (%)	FE	Experiment	Error (%)
Steel compressive strain	με	1413	1614	12.5	1463	1663	12.0
Steel tensile strain	με	7685	6630	15.9	7023	6118	14.8
Concrete compressive strain	με	5437	5065	7.3	3890	3458	12.5
Mid-span displacement	mm	11.5	10.2	12.7	41.3	40.0	3.3
Mean	%			12.1			10.7

4.4 Damage cloud

The Concrete Damaged Plasticity Model (CDPM) is widely recognized for its reliability and practical application in simulating concrete behavior under explosive conditions [31]. It integrates the flow theory of plasticity with damage mechanics to analyze the response of concrete structures [49]. The model features two independent damage variables, Dc and Dt, which assess the extent of damage

within the concrete. These variables are determined based on predefined plastic strains and field variables, with values ranging from 0 to 1, indicating the level of damage [35]. The CDPM also includes several additional parameters such as uniaxial compressive equivalent plastic strain (PEEQ), equivalent plastic strain rate (PEEQR) and scalar stiffness degradation variables (SDEG). which improve the model's performance under dynamic loading conditions [31]. Fig. 10 represents the contours for damaged variables for the 3 m span RC beam subjected to the No. 3 blast. The analysis, utilizing Dc and Dt values, accurately predicted both the damage extent and concentration. Observed spalling occurs in the top centeral region of the RC beam, while cracks initiate from the bottom span of the beam and extend upwards due to the explosive shock wave, consistent with the experimental results.

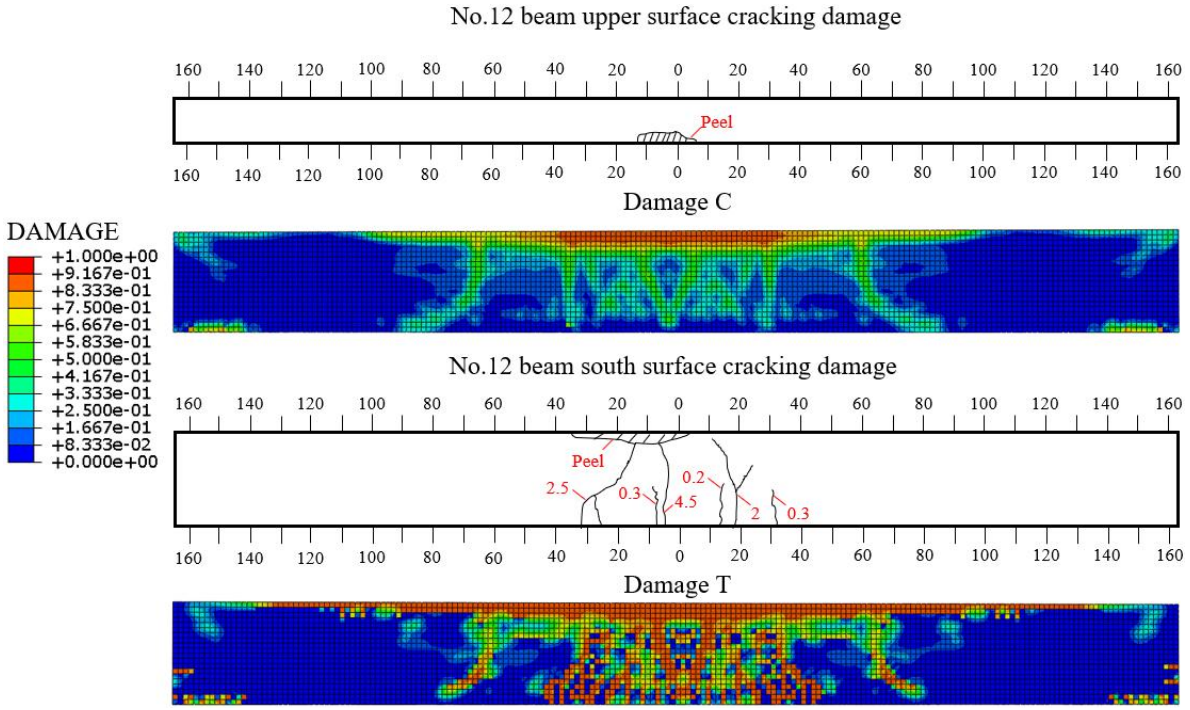


Fig. 10 Comparison of RC beam damage between test and FE simulation.

5. Conclusion

The size effect of reinforced concrete beams (RC beams) with different spans has been investigated through a series of overlying soil explosion experiments. The investigation began by analyzing the compressive and tensile strains of rebars within RC beams under three kinds of equivalent explosions, followed by an assessment of concrete compressive strain. Subsequently, the mid-span displacement of RC beams was analyzed, and numerical modelling techniques were used to characterize the failure

modes of RC beams. The purpose of this study is to provide a design basis for selecting appropriate laboratory scales for overlying soil explosion tests. The following conclusions can be drawn:

(1) The damage degree of RC beams increases with size; full-size RC beams exhibit larger crack lengths and widths compared to scaled models, demonstrating a pronounced size effect under overlying soil explosion conditions.

(2) During overlying soil explosion test, the pressure and positive pressure duration on the surface of the specimens vary due to the energy absorption effect of the overlying soil, even at a consistent scaled distance.

(3) The authors recommend that the scale ratio should be greater than 1/4 of the actual structures for overlying soil explosion tests. The mid-span displacement of scaled specimens differs substantially from that of the actual structures, indicating the need for further analysis.

(4) The use of identical parameters in FE may not accurately capture the size effect, resulting in potential errors. Recalibration of material parameters is necessary for full-size specimens with additional defects and pores, which necessitates collaborative efforts from researchers.

Acknowledgements

The project supported by the Young Scientists Fund of the National Natural Science Foundation of China (No.52408187).

Conflict of Interest

The authors declare that they have no known competing financial interests or personal relationships that could have appeared to influence the work reported in this paper.

Credit author statement

Shaohua Cao: Supervision, Validation. **Chunxiao Zhang**: Conceptualization, Validation. **Runze Cai**: Conceptualization, Data curation, Funding acquisition, Writing-Original draft preparation, Writing-review & editing.

References

[1] Shan T, Li Z, Jia H, Wang E, Niu Y, Zhang X et al. Investigation of tunnel size effects on rockburst

behaviors using electric potential monitoring under true triaxial loading conditions. Tunnelling and Underground Space Technology. 2026;167:107057.

[2] Cai R, Li Y, Zhang C, Cao H, Qi H, Mao J. Size effect on reinforced concrete slabs under direct contact explosion. Engineering Structures. 2022;252:113656.

[3] Zheng Z, Zeng C, Tian C, Wei X. Mesoscale numerical investigation on the size effect of concrete uniaxial compressive strength under different contact friction. Construction and Building Materials. 2022;346:128416.

[4] Kang G, Zhang Y, Xie X, Gu W. Investigation of blasting effects and mechanisms on concrete frustums under side-contact explosions. Defence Technology. 2025;49:113-27.

[5] Kargari A, Akhaveissy AH, Pietruszczak S. Experimental and meso-scale investigation of size effect on fracture properties in three-point concrete beams (TPB). Theoretical and Applied Fracture Mechanics. 2023;127:104026.

[6] Zhou FP, Balendran RV, Jeary AP. Size effect on flexural, splitting tensile, and torsional strengths of high-strength concrete. Cement and Concrete Research. 1998;28:1725-36.

[7] Zheng Y, Zhang Y, Zhuo J, Zhang P, Hu S. Mesoscale synergistic effect mechanism of aggregate grading and specimen size on compressive strength of concrete with large aggregate size. Construction and Building Materials. 2023;367:130346.

[8] Liu Y, Wu T, Wei H, Liu X, Pan Y. Size effect on tensile strength of lightweight aggregate concrete: A numerical investigation. Construction and Building Materials. 2022;323:126541.

[9] Jin L, Wan S, Li D, Miao L, Du X. Influence of concrete strength and aggregate size on the size effect of shear capacity of RC beam-column joints under monotonic loading: Mesoscale numerical tests. Structures. 2022;37:671-85.

[10] Yang X, Wu T, Liu X, Liu Y. Influence of web reinforcement on shear behavior and size effect of lightweight aggregate concrete deep beams: Experimental and theoretical studies. Engineering Structures. 2025;322:119119.

[11] Cucuzza R, Aloisio A, Accornero F, Marinelli A, Bassoli E, Marano GC. Size-scale effects and

418 modelling issues of fibre-reinforced concrete beams. Construction and Building Materials.
419 2023;392:131727.
420 [12] Lei Y, Jin L, Li D, Zhu H, Du X. Comparison of torsional damage and size effects of BFRP- and
421 steel-reinforced concrete beams with different stirrup ratios. Engineering Structures. 2023;285:116042.
422 [13] Fan S, Lim TYD, Teng S, Hai Tan K. Size effect of large high strength concrete beams with or
423 without shear reinforcement. Engineering Structures. 2023;281:115733.
424 [14] Li S-Z, Zhou X-H, Gao Y, Wang Y-H, Gan D, Ren W et al. Damage detection of concrete segment
425 in steel-concrete hybrid wind turbine tower. Structures. 2023;56:105009.
426 [15] Q. Yan, M. Hong, N. Zuo, G. Li, Q. Wang, Q. Wang. Study on the law of stress wave attenuation
427 in UHPC-sand composite protective layers under explosive loading. Protective Engineering. 2025; 47
428 (5), 10-17. (In Chinese).
429 [16] Y. Mu, Y. Zhang, S. Cheng, Research on dynamic response of steel fiber reinforced concrete and
430 constitutive model based on SHPB test, Protective Engineering. 2025;47 (6), 15-22. (In Chinese).
431 [17] Yang Y, Wu C, Liu Z. Rate dependent behaviour of 3D printed ultra-high performance fibre-
432 reinforced concrete under dynamic splitting tensile. Composite Structures. 2023;309:116727.
433 [18] Cheng JS, Wen HM, Cui ST, Zhang YL. Size effect of reinforced concrete beams under explosive
434 loadings-An experimental and numerical study. International Journal of Impact Engineering.
435 2025;198:105207.
436 [19] Jin L, Lu K, Lei Y, Du X, Yu W. Dynamic size effect in shear behavior of BFRP reinforced concrete
437 beams without stirrups with different shear-span ratios. International Journal of Impact Engineering.
438 2022;161:104103.
439 [20] Park JY, Krauthammer T. Development of an LEFM dynamic crack criterion for correlated size
440 and rate effects in concrete beams. International Journal of Impact Engineering. 2009;36:92-7.
441 [21] Cai RZ, Li YZ, Zhang CX, Cao H, Qi H, Mao JZ. Size effect on reinforced concrete slabs under
442 direct contact explosion. Engineering Structures. 2022;252.
443 [22] Mohamed OA, Kewalramani MA, Imran AM. Shear and flexure of FRP-reinforced concrete beams

444 and slabs – A review. Materials Today: Proceedings. 2023.
445 [23] Zhao Z, Cheng X, Li Y, Diao M, Guan H, An Y. Progressive collapse analysis of precast reinforced
446 concrete beam-column assemblies with different dry connections. Engineering Structures.
447 2023;287:116174.
448 [24] Cai R, Li Y, Zhang C, Qi H, Mao J, Pan Y et al. Damage assessment of prefabricated prestressed
449 channel slab under plane charge blast. Engineering Structures. 2021;246:113021.
450 [25] Patel M, Patel S. Effect of honeycomb cell size on the air-blast performance of sandwich panels.
451 Materials Today: Proceedings. 2023;78:792-7.
452 [26] Li C, Aoude H. Influence of UHPFRC jacketing on the static, blast and post-blast behaviour of
453 doubly-reinforced concrete beams. International Journal of Impact Engineering. 2023;179:104656.
454 [27] Das N, Nanthagopalan P. State-of-the-art review on ultra high performance concrete - Ballistic and
455 blast perspective. Cement and Concrete Composites. 2022;127:104383.
456 [28] Xu Y, Huang F, Liu Y, Yan J, Bai F, Yu H et al. Effect of close-in successive explosions on the
457 blast behaviors of reinforced concrete beams: An experimental study. Structures. 2023;53:29-46.
458 [29] Masi F, Stefanou I, Maffi-Berthier V. Scaling laws for the rigid-body response of masonry
459 structures under blast loads. Journal of Engineering Mechanics. 2020;147.
460 [30] Song D, Tan Q, Cao YYY, Hu Y. Experimental investigation on blast and post-blast performance
461 of reinforced concrete straight-wall arches strengthened with polyurea coating. Construction and
462 Building Materials. 2023;385:131352.
463 [31] Anas SM, Alam M, Umair M. Reinforced cement concrete (RCC) shelter and prediction of its blast
464 loads capacity. Materials Today: Proceedings. 2023;74:547-68.
465 [32] Tahzeeb R, Alam M, Muddassir SM. A comparative performance of columns: reinforced concrete,
466 composite, and composite with partial C-FRP wrapping under contact blast. Materials Today:
467 Proceedings. 2022;62:2191-202.
468 [33] Keskin İ, Yadgar Ahmed M, Ramadhan Taher N, Gör M, Zrar Abdulsamad B. An evaluation on
469 effects of surface explosion on underground tunnel; availability of ABAQUS Finite element method.

Tunnelling and Underground Space Technology. 2022;120:104306.

[34] Anas SM, Shariq M, Alam M. Performance of axially loaded square RC columns with single/double confinement layer(s) and strengthened with C-FRP wrapping under close-in blast. Materials Today: Proceedings. 2022;58:1128-41.

[35] Kumar V, Kartik KV, Iqbal MA. Experimental and numerical investigation of reinforced concrete slabs under blast loading. Engineering Structures. 2020;206:110125.

[36] Shamim S, Ahmad S, Khan RA. Numerical study on dynamic response of hollow and cavity type clay brick masonry infill panels subjected to blast loading. Engineering Failure Analysis. 2023;146:107104.

[37] Nguyen TNH, Tan K-H, Kanda T. Investigations on web-shear behavior of deep precast, prestressed concrete hollow core slabs. Engineering Structures. 2019;183:579-93.

[38] Tahzeeb R, Alam M, Muddassir SM. Performance of composite and tubular columns under close-in blast loading: A comparative numerical study. Materials Today: Proceedings. 2022;65:51-62.

[39] Shariq M, Saifi F, Alam M, Anas SM. Effect of concrete strength on the dynamic behavior of axially loaded reinforced concrete column subjected to close-range explosive loading. Materials Today: Proceedings. 2023;87:1-8.

[40] Hafezolghorani M, Hejazi F, Vaghei R, Jaafar MSB, Karimzade K. Simplified Damage Plasticity Model for Concrete. Structural Engineering International. 2017;27:68-78.

[41] SIMULIA. ABAQUS Analysis User's Manual Version 6.13 2023.

[42] Jiang Z, Zheng W, Wang Y, Sun P, Lu D, Sun L. The use of soundless chemical demolition agents in reinforced concrete deep beam demolition: Experimental and numerical study. Journal of Building Engineering. 2023;69:106260.

[43] Li Y, Chen Z, Ren X, Tao R, Gao R, Fang D. Experimental and numerical study on damage mode of RC slabs under combined blast and fragment loading. International Journal of Impact Engineering. 2020;142:103579.

[44] Jayasinghe LB, Thambiratnam DP, Perera N, Jayasooriya JHAR. Blast response of reinforced

concrete pile using fully coupled computer simulation techniques. Computers & Structures. 2014;135:40-9.

[45] Goel MD, Verma S, Mandal J, Panchal S. Effect of blast inside tunnel on surrounding soil mass, tunnel lining, and superstructure for varying shapes of tunnels. Underground Space. 2021;6:619-35.

[46] Goel MD, Chakraborty T, Matsagar VA. Dynamic Response of Steel-Sand Composite Stiffened Plates Under Blast Loading. In: Chakraborty S, Bhattacharya G, editors. Proceedings of the International Symposium on Engineering under Uncertainty: Safety Assessment and Management (ISEUSAM - 2012). India: Springer India; 2013. p. 787-803.

[47] Dobratz, B. M. (1981). LLNL explosives handbook: properties of chemical explosives and explosives and explosive simulants (No. UCRL-52997). Lawrence Livermore National Lab, CA (USA).

[48] Li S, Zhang Y, Feng S. Void detection and void defect control methods for large-scale immersed steel shell–concrete tunnels. Tunnelling and Underground Space Technology. 2023;134:105006.

[49] Wang Y, Chen Q, Zhao Z, Qiang H, Yang K, Wang X. Design and performance evaluation framework for seismically isolated reinforcement concrete columns subjected to blast loads. Structures. 2022;45:2239-52.

Supplementary Files

This is a list of supplementary files associated with this preprint. Click to download.

- Supplementarymaterial.docx